Measurements of the Angular Distributions in the Decays $B \to K^{(*)}\mu^+\mu^-$ at CDF

T. Aaltonen,[21] B. Álvarez González,[9,w] S. Amerio,[42a] D. Amidei,[32] A. Anastassov,[36] A. Annovi,[17] J. Antos,[12] G. Apollinari,[15] J. A. Appel,[15] A. Apresyan,[44] T. Arisawa,[51] A. Artikov,[13] J. Asaadi,[48] W. Ashmanskas,[15] B. Auerbach,[54] A. Aurisano,[48] F. Azfar,[40] W. Badgett,[15] A. Barbaro-Galtieri,[26] V. E. Barnes,[44] B. A. Barnett,[23] P. Barria,[45c,45a] P. Bartos,[12] M. Bauce,[42b,42a] G. Bauer,[30] F. Bedeschi,[45a] D. Beecher,[28] S. Behari,[23] G. Bellettini,[45b,45a] J. Bellinger,[53] D. Benjamin,[14] A. Beretvas,[15] A. Bhatti,[46] M. Binkley,[15,a] D. Bisello,[42b,42a] I. Bizjak,[28,cc] K. R. Bland,[5] C. Blocker,[6] B. Blumenfeld,[23] A. Bocci,[14] A. Bodek,[45] D. Bortoletto,[44] J. Boudreau,[43] A. Boveia,[11] B. Brau,[15,b] L. Brigliadori,[6b,6a] A. Brisuda,[12] C. Bromberg,[33] E. Brucken,[21] M. Bucciantonio,[45b,45a] J. Budagov,[13] H. S. Budd,[45] S. Budd,[22] K. Burkett,[15] G. Busetto,[42b,42a] P. Bussey,[19] A. Buzatu,[31] S. Cabrera,[14,y] C. Calancha,[29] S. Camarda,[4] M. Campanelli,[33] M. Campbell,[32] F. Canelli,[11,15] A. Canepa,[42] B. Carls,[22] D. Carlsmith,[53] R. Carosi,[45a] S. Carrillo,[16,l] S. Carron,[15] B. Casal,[9] M. Casarsa,[15] A. Castro,[6b,6a] P. Catastini,[15] D. Cauz,[53a] V. Cavaliere,[45c,45a] M. Cavalli-Sforza,[4] A. Cerri,[26,g] L. Cerrito,[28,r] Y. C. Chen,[1] M. Chertok,[7] G. Chiarelli,[45a] G. Chlachidze,[15] F. Chlebana,[15] K. Cho,[25] D. Chokheli,[13] J. P. Chou,[20] W. H. Chung,[53] Y. S. Chung,[45] C. I. Ciobanu,[41] M. A. Ciocci,[45c,45a] A. Clark,[18] D. Clark,[6] G. Compostella,[42b,42a] M. E. Convery,[15] J. Conway,[7] M. Corbo,[41] M. Cordelli,[17] C. A. Cox,[7] D. J. Cox,[7] F. Crescioli,[45b,45a] C. Cuenca Almenar,[54] J. Cuevas,[9,w] R. Culbertson,[15] D. Dagenhart,[15] N. d'Ascenzo,[41,u] M. Datta,[15] P. de Barbaro,[45] S. De Cecco,[50a] G. De Lorenzo,[4] M. Dell'Orso,[45b,45a] C. Deluca,[4] L. Demortier,[46] J. Deng,[14,d] M. Deninno,[6a] F. Devoto,[21] M. d'Errico,[42b,42a] A. Di Canto,[45b,45a] B. Di Ruzza,[45a] J. R. Dittmann,[5] M. D'Onofrio,[27] S. Donati,[45b,45a] P. Dong,[15] T. Dorigo,[42a] K. Ebina,[51] A. Elagin,[48] A. Eppig,[32] R. Erbacher,[7] D. Errede,[22] S. Errede,[22] N. Ershaidat,[41,bb] R. Eusebi,[48] H. C. Fang,[26] S. Farrington,[40] M. Feindt,[24] J. P. Fernandez,[29] C. Ferrazza,[45d,45a] R. Field,[16] G. Flanagan,[44,s] R. Forrest,[7] M. J. Frank,[5] M. Franklin,[20] J. C. Freeman,[15] I. Furic,[16] M. Gallinaro,[46] J. Galyardt,[10] J. E. Garcia,[18] A. F. Garfinkel,[44] P. Garosi,[45c,45a] H. Gerberich,[22] E. Gerchtein,[15] S. Giagu,[50b,50a] V. Giakoumopoulou,[3] P. Giannetti,[45a] K. Gibson,[43] C. M. Ginsburg,[15] N. Giokaris,[3] P. Giromini,[17] M. Giunta,[45a] G. Giurgiu,[23] V. Glagolev,[13] D. Glenzinski,[15] M. Gold,[35] D. Goldin,[48] N. Goldschmidt,[16] A. Golossanov,[15] G. Gomez,[9] G. Gomez-Ceballos,[30] M. Goncharov,[30] O. González,[29] I. Gorelov,[35] A. T. Goshaw,[14] K. Goulianos,[46] A. Gresele,[42a] S. Grinstein,[4] C. Grosso-Pilcher,[11] R. C. Group,[15] J. Guimaraes da Costa,[20] Z. Gunay-Unalan,[33] C. Haber,[26] S. R. Hahn,[15] E. Halkiadakis,[47] A. Hamaguchi,[39] J. Y. Han,[45] F. Happacher,[17] K. Hara,[49] D. Hare,[47] M. Hare,[50] R. F. Harr,[52] K. Hatakeyama,[5] C. Hays,[40] M. Heck,[24] J. Heinrich,[42] M. Herndon,[53] S. Hewamanage,[5] D. Hidas,[47] A. Hocker,[15] W. Hopkins,[15,h] D. Horn,[24] S. Hou,[1] R. E. Hughes,[37] M. Hurwitz,[11] U. Husemann,[54] N. Hussain,[31] M. Hussein,[33] J. Huston,[33] G. Introzzi,[45a] M. Iori,[50b,50a] A. Ivanov,[7,p] E. James,[15] D. Jang,[10] B. Jayatilaka,[14] E. J. Jeon,[25] M. K. Jha,[6a] S. Jindariani,[15] W. Johnson,[7] M. Jones,[44] K. K. Joo,[25] S. Y. Jun,[10] T. R. Junk,[15] T. Kamon,[48] P. E. Karchin,[52] Y. Kato,[39,o] W. Ketchum,[11] J. Keung,[42] V. Khotilovich,[48] B. Kilminster,[15] D. H. Kim,[25] H. S. Kim,[25] H. W. Kim,[25] J. E. Kim,[25] M. J. Kim,[17] S. B. Kim,[25] S. H. Kim,[49] Y. K. Kim,[11] N. Kimura,[51] S. Klimenko,[16] K. Kondo,[51] D. J. Kong,[25] J. Konigsberg,[16] A. Korytov,[16] A. V. Kotwal,[14] M. Kreps,[24] J. Kroll,[42] D. Krop,[11] N. Krumnack,[5,m] M. Kruse,[14] V. Krutelyov,[48,e] T. Kuhr,[24] M. Kurata,[49] S. Kwang,[11] A. T. Laasanen,[44] S. Lami,[45a] S. Lammel,[15] M. Lancaster,[28] R. L. Lander,[7] K. Lannon,[37,v] A. Lath,[47] G. Latino,[45c,45a] I. Lazzizzera,[42a] T. LeCompte,[2] E. Lee,[48] H. S. Lee,[11] J. S. Lee,[25] S. W. Lee,[48,x] S. Leo,[45b,45a] S. Leone,[45a] J. D. Lewis,[15] C.-J. Lin,[26] J. Linacre,[40] M. Lindgren,[15] E. Lipeles,[42] A. Lister,[18] D. O. Litvintsev,[15] C. Liu,[43] Q. Liu,[44] T. Liu,[15] S. Lockwitz,[54] N. S. Lockyer,[42] A. Loginov,[54] D. Lucchesi,[42b,42a] J. Lueck,[24] P. Lujan,[26] P. Lukens,[15] G. Lungu,[46] J. Lys,[26] R. Lysak,[12] R. Madrak,[15] K. Maeshima,[15] K. Makhoul,[30] P. Maksimovic,[23] S. Malik,[46] G. Manca,[27,c] A. Manousakis-Katsikakis,[3] F. Margaroli,[44] C. Marino,[24] M. Martínez,[4] R. Martínez-Ballarín,[29] P. Mastrandrea,[50a] M. Mathis,[23] M. E. Mattson,[52] P. Mazzanti,[6a] K. S. McFarland,[45] P. McIntyre,[48] R. McNulty,[27,j] A. Mehta,[27] P. Mehtala,[21] A. Menzione,[45a] C. Mesropian,[46] T. Miao,[15] D. Mietlicki,[32] A. Mitra,[1] H. Miyake,[49] S. Moed,[20] N. Moggi,[6a] M. N. Mondragon,[15,l] C. S. Moon,[25] R. Moore,[15] M. J. Morello,[15] J. Morlock,[24] P. Movilla Fernandez,[15] A. Mukherjee,[15] Th. Muller,[24] P. Murat,[15] M. Mussini,[6b,6a] J. Nachtman,[15,n] Y. Nagai,[49] J. Naganoma,[51] I. Nakano,[38] A. Napier,[50] J. Nett,[53] C. Neu,[42,aa] M. S. Neubauer,[22] J. Nielsen,[26,f] L. Nodulman,[2] O. Norniella,[22] E. Nurse,[28] L. Oakes,[40] S. H. Oh,[14] Y. D. Oh,[25] I. Oksuzian,[16] T. Okusawa,[39] R. Orava,[21] L. Ortolan,[4] S. Pagan Griso,[42b,42a] C. Pagliarone,[53a] E. Palencia,[9,g] V. Papadimitriou,[15] A. A. Paramonov,[2] J. Patrick,[15] G. Pauletta,[53b,53a] M. Paulini,[10] C. Paus,[30] D. E. Pellett,[7] A. Penzo,[53a] T. J. Phillips,[14] G. Piacentino,[45a] E. Pianori,[42] J. Pilot,[37] K. Pitts,[22] C. Plager,[8] L. Pondrom,[53] K. Potamianos,[44] O. Poukhov,[13,a] F. Prokoshin,[13,z] A. Pronko,[15] F. Ptohos,[17,i] E. Pueschel,[10] G. Punzi,[45b,45a] J. Pursley,[53] A. Rahaman,[43] V. Ramakrishnan,[53] N. Ranjan,[44] I. Redondo,[29] P. Renton,[40] M. Rescigno,[50a] F. Rimondi,[6b,6a] L. Ristori,[45a,15] A. Robson,[19] T. Rodrigo,[9] T. Rodriguez,[42] E. Rogers,[22]

S. Rolli,[50] R. Roser,[15] M. Rossi,[53a] F. Ruffini,[45c,45a] A. Ruiz,[9] J. Russ,[10] V. Rusu,[15] A. Safonov,[48] W. K. Sakumoto,[45] L. Santi,[53b,53a] L. Sartori,[45a] K. Sato,[49] V. Saveliev,[41,u] A. Savoy-Navarro,[41] P. Schlabach,[15] A. Schmidt,[24] E. E. Schmidt,[15] M. P. Schmidt,[54,a] M. Schmitt,[36] T. Schwarz,[7] L. Scodellaro,[9] A. Scribano,[45c,45a] F. Scuri,[45a] A. Sedov,[44] S. Seidel,[35] Y. Seiya,[39] A. Semenov,[13] F. Sforza,[45b,45a] A. Sfyrla,[22] S. Z. Shalhout,[7] T. Shears,[27] P. F. Shepard,[43] M. Shimojima,[49,t] S. Shiraishi,[11] M. Shochet,[11] I. Shreyber,[34] A. Simonenko,[13] P. Sinervo,[31] A. Sissakian,[13,a] K. Sliwa,[50] J. R. Smith,[7] F. D. Snider,[15] A. Soha,[15] S. Somalwar,[47] V. Sorin,[4] P. Squillacioti,[15] M. Stanitzki,[54] R. St. Denis,[19] B. Stelzer,[31] O. Stelzer-Chilton,[31] D. Stentz,[36] J. Strologas,[35] G. L. Strycker,[32] Y. Sudo,[49] A. Sukhanov,[16] I. Suslov,[13] K. Takemasa,[49] Y. Takeuchi,[49] J. Tang,[11] M. Tecchio,[32] P. K. Teng,[1] J. Thom,[15,h] J. Thome,[10] G. A. Thompson,[22] E. Thomson,[42] P. Ttito-Guzmán,[29] S. Tkaczyk,[15] D. Toback,[48] S. Tokar,[12] K. Tollefson,[33] T. Tomura,[49] D. Tonelli,[15] S. Torre,[17] D. Torretta,[15] P. Totaro,[53b,53a] M. Trovato,[45d,45a] Y. Tu,[42] N. Turini,[45c,45a] F. Ukegawa,[49] S. Uozumi,[25] A. Varganov,[32] E. Vataga,[45d,45a] F. Vázquez,[16,l] G. Velev,[15] C. Vellidis,[3] M. Vidal,[29] I. Vila,[9] R. Vilar,[9] M. Vogel,[35] G. Volpi,[45b,45a] P. Wagner,[42] R. L. Wagner,[15] T. Wakisaka,[39] R. Wallny,[8] S. M. Wang,[1] A. Warburton,[31] D. Waters,[28] M. Weinberger,[48] H. Wenzel,[15] W. C. Wester III,[15] B. Whitehouse,[50] D. Whiteson,[42,d] A. B. Wicklund,[2] E. Wicklund,[15] S. Wilbur,[11] F. Wick,[24] H. H. Williams,[42] J. S. Wilson,[37] P. Wilson,[15] B. L. Winer,[37] P. Wittich,[15,h] S. Wolbers,[15] H. Wolfe,[37] T. Wright,[32] X. Wu,[18] Z. Wu,[5] K. Yamamoto,[39] J. Yamaoka,[14] T. Yang,[15] U. K. Yang,[11,q] Y. C. Yang,[25] W.-M. Yao,[26] G. P. Yeh,[15] K. Yi,[15,n] J. Yoh,[15] K. Yorita,[51] T. Yoshida,[39,k] G. B. Yu,[14] I. Yu,[25] S. S. Yu,[15] J. C. Yun,[15] A. Zanetti,[53a] Y. Zeng,[14] and S. Zucchelli[6b,6a]

(CDF Collaboration)

[1]*Institute of Physics, Academia Sinica, Taipei, Taiwan 11529, Republic of China*
[2]*Argonne National Laboratory, Argonne, Illinois 60439, USA*
[3]*University of Athens, 157 71 Athens, Greece*
[4]*Institut de Fisica d'Altes Energies, Universitat Autonoma de Barcelona, E-08193, Bellaterra (Barcelona), Spain*
[5]*Baylor University, Waco, Texas 76798, USA*
[6a]*Istituto Nazionale di Fisica Nucleare Bologna, I-40127 Bologna, Italy*
[6b]*University of Bologna, I-40127 Bologna, Italy*
[6]*Brandeis University, Waltham, Massachusetts 02254, USA*
[7]*University of California, Davis, Davis, California 95616, USA*
[8]*University of California, Los Angeles, Los Angeles, California 90024, USA*
[9]*Instituto de Fisica de Cantabria, CSIC-University of Cantabria, 39005 Santander, Spain*
[10]*Carnegie Mellon University, Pittsburgh, Pennsylvania 15213, USA*
[11]*Enrico Fermi Institute, University of Chicago, Chicago, Illinois 60637, USA*
[12]*Comenius University, 842 48 Bratislava, Slovakia; Institute of Experimental Physics, 040 01 Kosice, Slovakia*
[13]*Joint Institute for Nuclear Research, RU-141980 Dubna, Russia*
[14]*Duke University, Durham, North Carolina 27708, USA*
[15]*Fermi National Accelerator Laboratory, Batavia, Illinois 60510, USA*
[16]*University of Florida, Gainesville, Florida 32611, USA*
[17]*Laboratori Nazionali di Frascati, Istituto Nazionale di Fisica Nucleare, I-00044 Frascati, Italy*
[18]*University of Geneva, CH-1211 Geneva 4, Switzerland*
[19]*Glasgow University, Glasgow G12 8QQ, United Kingdom*
[20]*Harvard University, Cambridge, Massachusetts 02138, USA*
[21]*Division of High Energy Physics, Department of Physics, University of Helsinki and Helsinki Institute of Physics, FIN-00014, Helsinki, Finland*
[22]*University of Illinois, Urbana, Illinois 61801, USA*
[23]*The Johns Hopkins University, Baltimore, Maryland 21218, USA*
[24]*Institut für Experimentelle Kernphysik, Karlsruhe Institute of Technology, D-76131 Karlsruhe, Germany*
[25]*Center for High Energy Physics: Kyungpook National University, Daegu 702-701, Korea; Seoul National University, Seoul 151-742, Korea; Sungkyunkwan University, Suwon 440-746, Korea; Korea Institute of Science and Technology Information, Daejeon 305-806, Korea; Chonnam National University, Gwangju 500-757, Korea; Chonbuk National University, Jeonju 561-756, Korea*
[26]*Ernest Orlando Lawrence Berkeley National Laboratory, Berkeley, California 94720, USA*
[27]*University of Liverpool, Liverpool L69 7ZE, United Kingdom*
[28]*University College London, London WC1E 6BT, United Kingdom*
[29]*Centro de Investigaciones Energeticas Medioambientales y Tecnologicas, E-28040 Madrid, Spain*
[30]*Massachusetts Institute of Technology, Cambridge, Massachusetts 02139, USA*

[31]Institute of Particle Physics: McGill University, Montréal, Québec, Canada H3A 2T8; Simon Fraser University, Burnaby, British Columbia, Canada V5A 1S6; University of Toronto, Toronto, Ontario, Canada M5S 1A7; and TRIUMF, Vancouver, British Columbia, Canada V6T 2A3
[32]University of Michigan, Ann Arbor, Michigan 48109, USA
[33]Michigan State University, East Lansing, Michigan 48824, USA
[34]Institution for Theoretical and Experimental Physics, ITEP, Moscow 117259, Russia
[35]University of New Mexico, Albuquerque, New Mexico 87131, USA
[36]Northwestern University, Evanston, Illinois 60208, USA
[37]The Ohio State University, Columbus, Ohio 43210, USA
[38]Okayama University, Okayama 700-8530, Japan
[39]Osaka City University, Osaka 588, Japan
[40]University of Oxford, Oxford OX1 3RH, United Kingdom
[42a]Istituto Nazionale di Fisica Nucleare, Sezione di Padova-Trento, I-35131 Padova, Italy
[42b]University of Padova, I-35131 Padova, Italy
[41]LPNHE, Universite Pierre et Marie Curie/IN2P3-CNRS, UMR7585, Paris, F-75252 France
[42]University of Pennsylvania, Philadelphia, Pennsylvania 19104, USA
[45a]Istituto Nazionale di Fisica Nucleare Pisa, I-56127 Pisa, Italy
[45b]University of Pisa, I-56127 Pisa, Italy
[45c]University of Siena, I-56127 Pisa, Italy
[45d]Scuola Normale Superiore, I-56127 Pisa, Italy
[43]University of Pittsburgh, Pittsburgh, Pennsylvania 15260, USA
[44]Purdue University, West Lafayette, Indiana 47907, USA
[45]University of Rochester, Rochester, New York 14627, USA
[46]The Rockefeller University, New York, New York 10065, USA
[50a]Istituto Nazionale di Fisica Nucleare, Sezione di Roma 1, I-00185 Roma, Italy
[50b]Sapienza Università di Roma, I-00185 Roma, Italy
[47]Rutgers University, Piscataway, New Jersey 08855, USA
[48]Texas A&M University, College Station, Texas 77843, USA
[53a]Istituto Nazionale di Fisica Nucleare Trieste/Udine, I-34100 Trieste, I-33100 Udine, Italy
[53b]University of Trieste/Udine, I-33100 Udine, Italy
[49]University of Tsukuba, Tsukuba, Ibaraki 305, Japan
[50]Tufts University, Medford, Massachusetts 02155, USA
[51]Waseda University, Tokyo 169, Japan
[52]Wayne State University, Detroit, Michigan 48201, USA
[53]University of Wisconsin, Madison, Wisconsin 53706, USA
[54]Yale University, New Haven, Connecticut 06520, USA
(Received 2 August 2011; published 24 February 2012)

We report an indirect search for nonstandard model physics using the flavor-changing neutral current decays $B \to K^{(*)}\mu^+\mu^-$. We reconstruct the decays and measure their angular distributions, as a function of $q^2 = M^2_{\mu\mu}c^2$, where $M_{\mu\mu}$ is the dimuon mass, in $p\bar{p}$ collisions at $\sqrt{s} = 1.96$ TeV using a data sample corresponding to an integrated luminosity of 6.8 fb^{-1}. The transverse polarization asymmetry $A_T^{(2)}$ and the time-reversal-odd charge-and-parity asymmetry $A_{\rm im}$ are measured for the first time, together with the K^* longitudinal polarization fraction F_L and the muon forward-backward asymmetry $A_{\rm FB}$ for the decays $B^0 \to K^{*0}\mu^+\mu^-$ and $B^+ \to K^{*+}\mu^+\mu^-$. The $B \to K^*\mu^+\mu^-$ forward-backward asymmetry in the most sensitive kinematic regime, $1 \le q^2 < 6$ GeV$^2/c^2$, is measured to be $A_{\rm FB} = 0.29^{+0.20}_{-0.23}({\rm stat}) \pm 0.07({\rm syst})$, the most precise result to date. No deviations from the standard model predictions are observed.

DOI: 10.1103/PhysRevLett.108.081807 PACS numbers: 13.20.He, 11.30.Er

The decays $B \to K^{(*)}\mu^+\mu^-$ [1], which proceed via the flavor-changing neutral current process $b \to s\mu^+\mu^-$, are among the most promising probes of the standard model (SM) and its extensions [2]. These decays are suppressed in the SM, since they occur through higher order amplitudes involving quantum loops. Such amplitudes can receive competing contributions from unknown massive virtual particles or new couplings, which may significantly alter the decay kinematics with respect to the SM predictions. Multibody final states further enrich the phenomenology of these decays, offering sensitivity to a broad class of SM extensions through measurement of angular distributions as a function of $q^2 \equiv M^2_{\mu\mu}c^2$, where $M_{\mu\mu}$ is the dimuon invariant mass.

The full differential decay distribution for decays $B \to K^*(892)\mu^+\mu^- \to K\pi\mu^+\mu^-$ is described in terms of four kinematic variables: the angle θ_μ between the μ^+ (μ^-) direction and the direction opposite to the B ($\bar{B}$) meson in

the dimuon rest frame, the angle θ_K between the kaon direction and the direction opposite to the B meson in the K^* rest frame, the angle ϕ between the two planes formed by the dimuon and the K-π systems, and q^2. The decay distribution is a function of eight independent angular coefficients, each functions of q^2, that are physics observables to be determined experimentally. A simultaneous determination of all the coefficients requires signal event samples of much larger size than currently available. Following Refs. [3–6], we project the decay distribution into three simpler relations each involving just one of the angles:

$$\begin{aligned}\frac{1}{\Gamma}\frac{d\Gamma}{d\cos\theta_K} &= \frac{3}{2}F_L\cos^2\theta_K + \frac{3}{4}(1-F_L)(1-\cos^2\theta_K),\\ \frac{1}{\Gamma}\frac{d\Gamma}{d\cos\theta_\mu} &= \frac{3}{4}F_L(1-\cos^2\theta_\mu)\\ &\quad + \frac{3}{8}(1-F_L)(1+\cos^2\theta_\mu) + A_{\rm FB}\cos\theta_\mu,\\ \frac{1}{\Gamma}\frac{d\Gamma}{d\phi} &= \frac{1}{2\pi}\left[1+\frac{1}{2}(1-F_L)A_T^{(2)}\cos 2\phi + A_{\rm im}\sin 2\phi\right],\end{aligned} \tag{1}$$

where Γ is the partial decay width. These one-dimensional relations are functions of a subset of four angular observables, each of which depends on q^2: $A_{\rm FB}$, the muon forward-backward asymmetry; F_L, the K^* longitudinal polarization fraction; $A_T^{(2)}$, the transverse polarization asymmetry [3,5]; and $A_{\rm im}$, the time-reversal-odd charge-and-parity asymmetry (T-odd CP asymmetry) [4,6].

BABAR [7], Belle [8], and CDF [9] have reported measurements of $A_{\rm FB}$ and F_L in the $B \to K^*\ell^+\ell^-$ decay modes. All experiments find $A_{\rm FB}$ to be larger than the SM expectation, but so far none has had sufficient sensitivity to be conclusive. However, Belle reports that the cumulative difference of their measurement from the SM prediction corresponds to 2.7σ [8]. With the current sample, CDF has sensitivity comparable to Belle's. A similar discrepancy in CDF data would provide a strong indication of physics beyond the standard model (BSM).

In this Letter, we report measurements of F_L and $A_{\rm FB}$ and for the first time use the angle ϕ to access $A_T^{(2)}$ and $A_{\rm im}$ in the decay $B \to K^*\mu^+\mu^-$. We use a sample of $p\bar{p}$ collisions at a center-of-mass energy of $\sqrt{s} = 1.96$ TeV, corresponding to 6.8 fb^{-1} integrated luminosity collected with the CDF II detector. The measurement updates and supersedes an earlier analysis [9]. We include the $B^+ \to K^{*+}\mu^+\mu^-$ decay, reconstructed for the first time in hadronic collisions, and improve the $B^0 \to K^{*0}\mu^+\mu^-$ signal selection by 9% with almost the same background rejection, along with the added data. The resulting 82% increase in signal statistics reduces the uncertainties on $A_{\rm FB}$ and F_L by 50% and enables the first measurement of $A_T^{(2)}$ and $A_{\rm im}$. We also update the measurement of $A_{\rm FB}$ in $B^+ \to K^+\mu^+\mu^-$ decays. Measurements of branching ratios are reported in another Letter [10].

The differential decay distribution of $B \to K^*\mu^+\mu^-$ is calculated in an operator product expansion [11]. In the SM, only the Wilson coefficients $C_{7,9,10}^{\rm eff}$ are relevant. Each of the angular observables, which include different combinations of Wilson coefficients, has unique sensitivity to specific features of BSM models. The measurement of F_L could constrain BSM models in which couplings to the K^* helicity states are different from the SM ones [3]. The observables $A_{\rm FB}$, $A_T^{(2)}$, and $A_{\rm im}$ are especially sensitive, since the hadronic uncertainties cancel in the asymmetry. The asymmetry of the muon direction between the forward ($\cos\theta_\mu > 0$) and backward ($\cos\theta_\mu < 0$) directions in the dimuon rest frame, $A_{\rm FB}$, is expected to be small at low q^2 and large and positive at high q^2 in the SM. The BSM contributions can change the magnitude and the sign of $A_{\rm FB}$. The observables $A_T^{(2)}$ and $A_{\rm im}$ have recently been proposed as powerful probes of SM extensions that involve weak interactions of particles with positive chirality (right-handed currents).

In the SM, $A_T^{(2)}$ is accurately predicted to be approximately zero at low q^2 and negative at high q^2 [12]. However, a broad class of BSM models, which involve the CP-conserving right-handed currents, expect $A_T^{(2)}$ reaching values up to ± 1 [3,5,13]. The SM predicts $A_{\rm im}$ to be close to zero for all accessible values of q^2. Deviations could be observed in the case of CP-violating right-handed currents [6].

The $B^+ \to K^+\mu^+\mu^-$ angular distribution is simpler than the $B \to K^*\mu^+\mu^-$ distribution. Although $A_{\rm FB}$ is the only observable accessible in this decay, it provides complementary sensitivity to BSM models with respect to $B \to K^*\mu^+\mu^-$ measurements. The asymmetry expected in the SM is quite small over the entire range of q^2 [14] but could be enhanced if scalar- or tensor-type BSM contributions are present [13].

The reconstruction of the $B \to K^{(*)}\mu^+\mu^-$ decays starts with a dimuon sample selected by the online trigger system [15] of the CDF II detector [16]. The trigger uses information from muon detectors and the central drift tracking chamber [17]. The chamber provides 96 samplings of charged-particle's trajectories (tracks) between radii of 40 and 137 cm, allowing an accurate determination of particles' momenta. The central muon system (CMU) and the forward muon system drift chambers [18] cover the pseudorapidity regions $|\eta| < 0.6$ and $0.6 < |\eta| < 1.0$, respectively [19]. The central muon upgrade system is located radially behind the CMU and an additional steel absorber and covers $|\eta| < 0.6$. The dimuon trigger requires a pair of oppositely charged particles with momenta transverse to the beam line $p_T > 1.5$ GeV/c that are also identified in the CMU or forward muon system chambers. At least one of the muon tracks in the pair is required to be a CMU muon. The trigger also requires either of the

following criteria: The dimuon pair satisfies $L_{xy} > 100\ \mu$m, where the transverse decay length L_{xy} is the flight distance between the dimuon vertex and the event primary vertex projected onto the dimuon momentum vector, or one of the muon candidates has $p_T > 3.0$ GeV/c and is identified by both the CMU and central muon upgrade system chambers. The other detector subsystems relevant for this analysis are discussed in Ref. [20].

Each offline track is required to satisfy the standard quality requirements to ensure well-measured momenta and decay vertices [9]. The decay length and mass of each dimuon pair are calculated after a vertex fit. Dimuons are required to have q^2 values outside the ranges of $8.68 < q^2 < 10.09$ GeV$^2/c^2$ and $12.86 < q^2 < 14.18$ GeV$^2/c^2$ [9], to reject J/ψ and $\psi(2S)$ decays, typically reconstructed with 14 MeV/c^2 mass resolution. The dimuon pair is then combined with tracks forming a $K^{*0} \to K^+\pi^-$ candidate to form a $B^0 \to K^{*0}\mu^+\mu^-$ candidate or a $K^{*+} \to K^0_S(\to \pi^+\pi^-)\pi^+$ candidate to form a $B^+ \to K^{*+}\mu^+\mu^-$ candidate. Loose particle identification requirements are applied to the K^+ candidate [10]. The K^0_S, K^{*0}, and K^{*+} candidates are required to have masses consistent with the known values [21] and to have $p_T > 1$ GeV/c. The K^0_S is also required to decay in a vertex displaced from the dimuon vertex. In the K^{*0} reconstruction, we choose the $K^+\pi^-$ assignment that yields the mass closer to the known K^{*0} mass. This is correct 92% of the time, as shown by simulation. The reconstructed B candidates are required to have $p_T > 4$ GeV/c. To further optimize the selection, a neural network (NN) classifier [22] is trained for each channel using simulated signal and background sampled from B mass sidebands (0.1–0.36 GeV/c^2 higher than the known B mass [21]) in data. The optimized NN threshold is determined to minimize the statistical uncertainty of the angular observables, using 15–18 discriminating observables including p_T of B meson and daughter particles, K^* and K^0_S masses, vertex fit parameters, and muon identification quality [9]. No angular bias due to the choice of the NN threshold is found in simulation or in $B \to J/\psi(\to \mu^+\mu^-)K^{(*)}$ control samples.

The signal yield is obtained from an unbinned maximum likelihood fit to the mass distribution with a probability density function consisting of Gaussian distributions determined from simulation for the signal and a linear background. The 5.18–5.70 GeV/c^2 fit range avoids the 5.0–5.18 GeV/c^2 region, dominated by background from multibody B decays. The signal region is defined within ± 40 MeV/c^2 from the known B mass [21]. In this range, the contributions from similar decays such as $B^0 \to \rho^0\mu^+\mu^-$ and $B^+ \to \pi^+\mu^+\mu^-$ are negligible due to misreconstruction and rates smaller than our signal rates. The 1% $B^0_s \to \phi\mu^+\mu^-$ contamination to the $B^0 \to K^{*0}\mu^+\mu^-$ signal is included in the systematic uncertainties.

We find 234 ± 19 $B^+ \to K^+\mu^+\mu^-$, 164 ± 15 $B^0 \to K^{*0}\mu^+\mu^-$, and 20 ± 6 $B^+ \to K^{*+}\mu^+\mu^-$ events (Fig. 1).

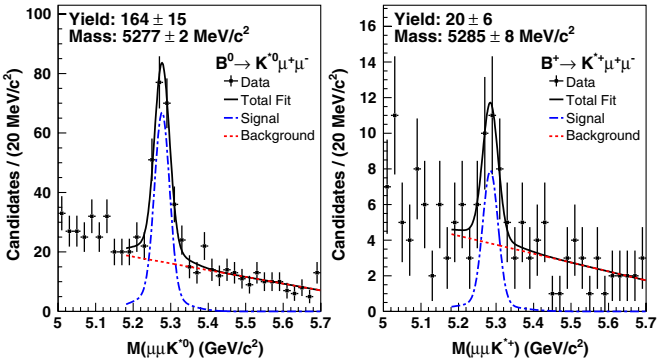

FIG. 1 (color online). Invariant mass of $B^0 \to K^{*0}\mu^+\mu^-$ (left) and $B^+ \to K^{*+}\mu^+\mu^-$ (right), with fit results overlaid.

The uncertainties are statistical only. We divide the events into six bins in q^2. Two semi-inclusive bins are included with ranges covering theoretically well-controlled regions. We obtain the signal yields (Tables I, II, and III) in the individual q^2 ranges by fitting the mass as described above.

To extract the quantities F_L, $A_{\rm FB}$, $A_T^{(2)}$, and $A_{\rm im}$, we perform likelihood fits to the distributions of $\cos\theta_K$, $\cos\theta_\mu$, and ϕ for candidates in each q^2 range and with B mass in the signal region. The signal fractions are fixed to the results of the mass fits. Signal probability density functions for angular distributions are formed from Eq. (1), including detector acceptance and the K-π interchange, estimated by using simulation. The incorrect K-π assignment in the $K^{*0} \to K^+\pi^-$ decay distorts the signal mass distribution and swaps the sign of $\cos\theta_\mu$. This is modeled with an additional signal-like term in the likelihood. The contribution from decays with nonresonant K-π pairs is expected to be small [3] and neglected in the fit. The angular probability density function for the background are modeled by using the same B mass sidebands used for NN training.

The values of F_L in individual q^2 ranges are extracted from fits to the $\cos\theta_K$ distributions and then used as fixed inputs in the fits of $A_{\rm FB}$, $A_T^{(2)}$, and $A_{\rm im}$. The asymmetry $A_{\rm FB}$ ($A_T^{(2)}$ and $A_{\rm im}$) is obtained from fits to the $\cos\theta_\mu$ (ϕ) distributions.

The $B^0 \to K^{*0}\mu^+\mu^-$ results [23] are listed in Table I, and the forward-backward asymmetry $A_{\rm FB}$ is illustrated in Fig. 2(a) as a function of q^2. To increase sensitivity, we also fit the combined $B^0 \to K^{*0}\mu^+\mu^-$ and $B^+ \to K^{*+}\mu^+\mu^-$ modes [23] (Table II and Fig. 3), assuming they have the same decay dynamics. The determinations of $A_{\rm FB}$ and F_L are among the most precise from a single experiment. However, the shape of the $A_{\rm FB}$ distribution as a function of q^2, which carries the majority of the discriminating information [12], does not deviate from the SM expectation and cannot yet provide conclusive discrimination between the SM and the inverted C_7 scenario which is suggested by the Belle results [8]. In the most sensitive kinematic regime, $1 \le q^2 < 6$ GeV$^2/c^2$, we find

TABLE I. Summary of $B^0 \to K^{*0}\mu^+\mu^-$ fit results. The first (second) uncertainty is statistical (systematic).

q^2 (GeV$^2/c^2$)	$N(K^{*0}\mu^+\mu^-)$	F_L	$A_{\rm FB}$	$A_T^{(2)}$	$A_{\rm im}$
[0.00, 2.00)	30.7 ± 4.7	$0.31^{+0.17}_{-0.16} \pm 0.02$	$-0.37^{+0.27}_{-0.32} \pm 0.11$	$-0.8 \pm 0.7 \pm 0.3$	$0.37^{+0.31}_{-0.33} \pm 0.08$
[2.00, 4.30)	14.2 ± 4.2	$0.35^{+0.26}_{-0.24} \pm 0.03$	$0.30^{+0.32}_{-0.36} \pm 0.17$	$1.4^{+2.0}_{-1.1} \pm 1.2$	$-0.80^{+0.48}_{-0.29} \pm 0.13$
[4.30, 8.68)	31.3 ± 7.4	$0.60^{+0.17}_{-0.18} \pm 0.05$	$-0.08^{+0.22}_{-0.21} \pm 0.03$	$1.8^{+1.6}_{-1.7} \pm 1.5$	$0.03^{+0.34}_{-0.34} \pm 0.06$
[10.09, 12.86)	38.4 ± 7.6	$0.40^{+0.16}_{-0.16} \pm 0.02$	$0.42^{+0.17}_{-0.21} \pm 0.10$	$-1.0^{+0.9}_{-0.8} \pm 0.5$	$0.47^{+0.26}_{-0.28} \pm 0.09$
[14.18, 16.00)	31.6 ± 4.7	$0.32^{+0.14}_{-0.14} \pm 0.03$	$0.40^{+0.18}_{-0.21} \pm 0.07$	$0.4 \pm 0.8 \pm 0.2$	$0.15^{+0.25}_{-0.26} \pm 0.01$
[16.00, 19.30)	20.7 ± 4.8	$0.16^{+0.22}_{-0.18} \pm 0.06$	$0.66^{+0.18}_{-0.26} \pm 0.19$	$-0.9 \pm 0.8 \pm 0.4$	$-0.30^{+0.36}_{-0.35} \pm 0.14$
[0.00, 4.30)	44.2 ± 6.5	$0.33^{+0.14}_{-0.14} \pm 0.02$	$-0.08^{+0.21}_{-0.20} \pm 0.05$	$-0.2 \pm 0.6 \pm 0.1$	$-0.02^{+0.28}_{-0.28} \pm 0.01$
[1.00, 6.00)	23.8 ± 6.5	$0.60^{+0.21}_{-0.23} \pm 0.09$	$0.36^{+0.46}_{-0.28} \pm 0.11$	$1.6^{+1.8}_{-1.9} \pm 2.2$	$-0.02^{+0.40}_{-0.40} \pm 0.03$

TABLE II. Summary of combined $B \to K^*\mu^+\mu^-$ fit results. $N(K^{*0}\mu^+\mu^-)$ is taken from Table I.

q^2 (GeV$^2/c^2$)	$N(K^{*+}\mu^+\mu^-)$	F_L	$A_{\rm FB}$	$A_T^{(2)}$	$A_{\rm im}$
[0.00, 2.00)	2.5 ± 1.6	$0.30^{+0.16}_{-0.16} \pm 0.02$	$-0.35^{+0.26}_{-0.23} \pm 0.10$	$-1.0^{+0.7}_{-0.6} \pm 0.4$	$0.21^{+0.30}_{-0.31} \pm 0.10$
[2.00, 4.30)	1.3 ± 1.8	$0.37^{+0.25}_{-0.24} \pm 0.10$	$0.29^{+0.32}_{-0.35} \pm 0.15$	$1.3^{+2.4}_{-1.2} \pm 0.9$	$-0.72^{+0.46}_{-0.36} \pm 0.21$
[4.30, 8.68)	3.9 ± 3.5	$0.68^{+0.15}_{-0.17} \pm 0.09$	$0.01^{+0.20}_{-0.20} \pm 0.09$	$3.4^{+1.9}_{-2.1} \pm 3.6$	$0.11^{+0.31}_{-0.32} \pm 0.09$
[10.09, 12.86)	6.0 ± 2.8	$0.47^{+0.14}_{-0.14} \pm 0.03$	$0.38^{+0.16}_{-0.19} \pm 0.09$	$-1.8^{+0.9}_{-0.8} \pm 0.8$	$0.32^{+0.25}_{-0.26} \pm 0.06$
[14.18, 16.00)	1.6 ± 1.8	$0.29^{+0.14}_{-0.13} \pm 0.05$	$0.44^{+0.18}_{-0.21} \pm 0.10$	$0.2 \pm 0.8 \pm 0.2$	$0.19^{+0.24}_{-0.26} \pm 0.04$
[16.00, 19.30)	4.1 ± 2.3	$0.20^{+0.19}_{-0.17} \pm 0.05$	$0.65^{+0.17}_{-0.18} \pm 0.16$	$-0.7 \pm 0.8 \pm 0.3$	$-0.20^{+0.33}_{-0.33} \pm 0.09$
[0.00, 4.30)	3.8 ± 2.4	$0.33^{+0.14}_{-0.13} \pm 0.03$	$-0.08^{+0.21}_{-0.20} \pm 0.05$	$-0.3 \pm 0.6 \pm 0.1$	$-0.10^{+0.27}_{-0.26} \pm 0.10$
[1.00, 6.00)	5.0 ± 3.0	$0.69^{+0.19}_{-0.21} \pm 0.08$	$0.29^{+0.20}_{-0.23} \pm 0.07$	$1.7 \pm 2.2 \pm 2.5$	$0.09^{+0.34}_{-0.35} \pm 0.18$

$A_{\rm FB} = 0.29^{+0.20}_{-0.23}(\text{stat}) \pm 0.07(\text{syst})$, consistent with the SM prediction of $A_{\rm FB}^{\rm SM} = 0.022 \pm 0.028$ [5] and the Belle result of $A_{\rm FB}^{\rm Belle} = 0.26^{+0.27}_{-0.30}(\text{stat}) \pm 0.07(\text{syst})$ [8]. The polarization in the same q^2 range, $F_L = 0.69^{+0.19}_{-0.21}(\text{stat}) \pm 0.08(\text{syst})$, is also consistent with the corresponding SM prediction, $F_L^{\rm SM} = 0.73^{+0.02}_{-0.03}$ [5] and the Belle result of $F_L^{\rm Belle} = 0.67 \pm 0.23(\text{stat}) \pm 0.05(\text{syst})$ [8].

Tables I and II and Figs. 3(c) and 3(d) show the results of the first measurement of $A_T^{(2)}$ and $A_{\rm im}$. These results explore new regions of BSM parameter space providing, in combination with other observables, initial discriminating information between different classes of BSM models.

In the $B^+ \to K^+\mu^+\mu^-$ fit for $A_{\rm FB}$ [23], we assume no scalar term [14] and set $F_L = 1$ in Eq. (1). The results are the most precise from a single experiment and are consistent with the SM predictions [Fig. 2(b) and Table III].

TABLE III. Summary of $B^+ \to K^+\mu^+\mu^-$ fit results.

q^2 (GeV$^2/c^2$)	$N(K^+\mu^+\mu^-)$	$A_{\rm FB}$
[0.00, 2.00)	18.6 ± 5.6	$0.13^{+0.42}_{-0.43} \pm 0.07$
[2.00, 4.30)	40.3 ± 6.7	$0.32^{+0.15}_{-0.16} \pm 0.05$
[4.30, 8.68)	68.5 ± 10.5	$0.01^{+0.13}_{-0.10} \pm 0.01$
[10.09, 12.86)	43.5 ± 7.1	$-0.03^{+0.11}_{-0.10} \pm 0.04$
[14.18, 16.00)	35.9 ± 5.7	$-0.05^{+0.09}_{-0.11} \pm 0.03$
[16.00, 23.00)	28.9 ± 6.3	$0.09^{+0.17}_{-0.13} \pm 0.03$
[0.00, 4.30)	57.8 ± 8.8	$0.31^{+0.16}_{-0.16} \pm 0.04$
[1.00, 6.00)	74.5 ± 9.6	$0.13^{+0.09}_{-0.09} \pm 0.02$

The sources of systematic uncertainty include the estimation of detector acceptance, signal fraction estimation and shape modeling of events in the signal window, feed-down background from other B decays, trigger efficiency and bias modeling, incorrect K-π assignment in the $K^{*0} \to K^+\pi^-$ decay, and fitting bias. The largest contributions to $A_{\rm FB}$, F_L, and $A_{\rm im}$ are from uncertainties on the signal

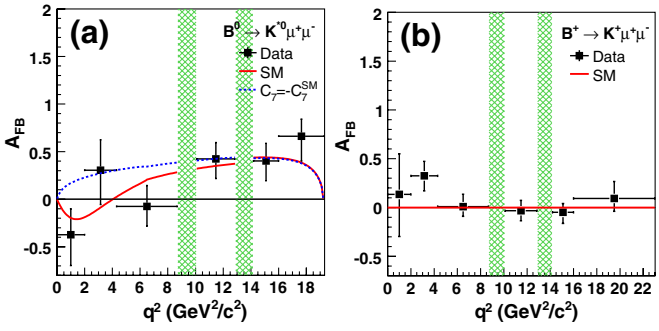

FIG. 2 (color online). Measurements of forward-backward asymmetry $A_{\rm FB}$ in the decay (a) $B^0 \to K^{*0}\mu^+\mu^-$ and (b) $B^+ \to K^+\mu^+\mu^-$ as a function of dimuon mass squared q^2. Points are the fit results from the data. The solid curves are the SM expectation [24]. The dotted curve is the $C_7 = -C_7^{\rm SM}$ expectation suggested by some BSM models. Hatched regions are excluded resonant (charmonium) decay regions.

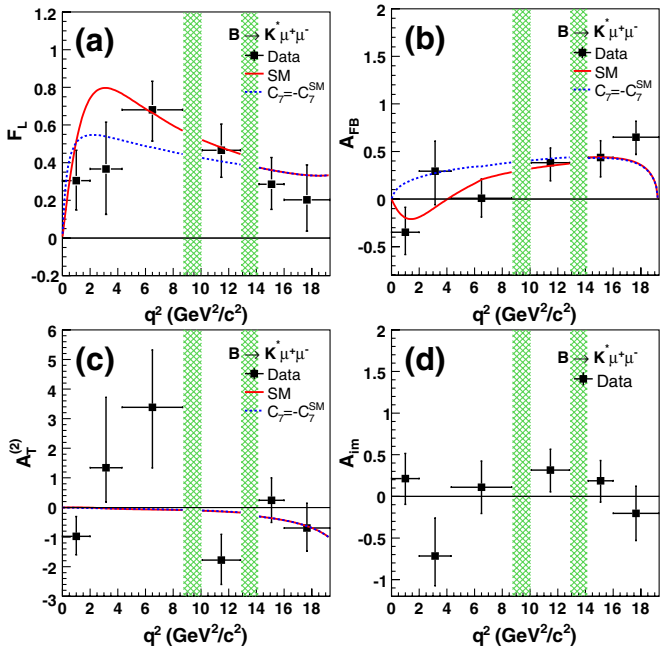

FIG. 3 (color online). Measurements of (a) longitudinal K^* polarization fraction F_L, (b) forward-backward asymmetry $A_{\rm FB}$, (c) transverse polarization asymmetry $A_T^{(2)}$, and (d) T-odd CP asymmetry $A_{\rm im}$ in the combined decay mode $B \to K^* \mu^+ \mu^-$.

fraction in the signal window. For the $A_{\rm FB}$, $A_T^{(2)}$, and $A_{\rm im}$ measurements, we also consider the additional uncertainty from the statistical uncertainty on F_L, which gives the largest contribution to the $A_T^{(2)}$ uncertainty.

In summary, we have reconstructed the decays $B^0 \to K^{*0} \mu^+ \mu^-$ and $B^+ \to K^{*+} \mu^+ \mu^-$ and report the measurements of the three one-dimensional projections of their full angular distributions. The decay $B^+ \to K^{*+} \mu^+ \mu^-$ is reconstructed for the first time in hadron collisions. We have measured the muon forward-backward asymmetry $A_{\rm FB}$, the K^* longitudinal polarization fraction F_L, the transverse polarization asymmetry $A_T^{(2)}$, and the T-odd CP asymmetry $A_{\rm im}$ as a function of q^2. Measurements of $A_T^{(2)}$ and $A_{\rm im}$ are reported for the first time. We also have measured $A_{\rm FB}$ by using the decay $B^+ \to K^+ \mu^+ \mu^-$. All results are among the most precise from a single experiment to date. We do not observe a discrepancy from the SM as reported by Belle, although our results are consistent with all recent measurements from B-factory experiments [7,8].

We thank C. Bobeth, J. Matias, and W. Altmannshofer for valuable suggestions. Our special gratitude goes to D. van Dyk, who provided the tool to obtain theoretical predictions. We thank the Fermilab staff and the technical staffs of the participating institutions for their vital contributions. This work was supported by the U.S. Department of Energy and National Science Foundation; the Italian Istituto Nazionale di Fisica Nucleare; the Ministry of Education, Culture, Sports, Science and Technology of Japan; the Natural Sciences and Engineering Research Council of Canada; the National Science Council of the Republic of China; the Swiss National Science Foundation; the A. P. Sloan Foundation; the Bundesministerium für Bildung und Forschung, Germany; the Korean World Class University Program, the National Research Foundation of Korea; the Science and Technology Facilities Council and the Royal Society, United Kingdom; the Institut National de Physique Nucleaire et Physique des Particules/CNRS; the Russian Foundation for Basic Research; the Ministerio de Ciencia e Innovación, and Programa Consolider-Ingenio 2010, Spain; the Slovak R&D Agency; and the Academy of Finland.

[a]Deceased.
[b]Visitor from University of Massachusetts Amherst, Amherst, MA 01003, USA.
[c]Visitor from Istituto Nazionale di Fisica Nucleare, Sezione di Cagliari, 09042 Monserrato (Cagliari), Italy.
[d]Visitor from University of California Irvine, Irvine, CA 92697, USA.
[e]Visitor from University of California Santa Barbara, Santa Barbara, CA 93106, USA.
[f]Visitor from University of California Santa Cruz, Santa Cruz, CA 95064, USA.
[g]Visitor from CERN, CH-1211 Geneva, Switzerland.
[h]Visitor from Cornell University, Ithaca, NY 14853, USA.
[i]Visitor from University of Cyprus, Nicosia CY-1678, Cyprus.
[j]Visitor from University College Dublin, Dublin 4, Ireland.
[k]Visitor from University of Fukui, Fukui City, Fukui Prefecture, Japan 910-0017.
[l]Visitor from Universidad Iberoamericana, Mexico D.F., Mexico.
[m]Visitor from Iowa State University, Ames, IA 50011, USA.
[n]Visitor from University of Iowa, Iowa City, IA 52242, USA.
[o]Visitor from Kinki University, Higashi-Osaka City, Japan 577-8502.
[p]Visitor from Kansas State University, Manhattan, KS 66506, USA.
[q]Visitor from University of Manchester, Manchester M139PL, United Kingdom.
[r]Visitor from Queen Mary, University of London, London, E1 4NS, United Kingdom.
[s]Visitor from Muons, Inc., Batavia, IL 60510, USA.
[t]Visitor from Nagasaki Institute of Applied Science, Nagasaki, Japan.
[u]Visitor from National Research Nuclear University, Moscow, Russia.
[v]Visitor from University of Notre Dame, Notre Dame, IN 46556, USA.
[w]Visitor from Universidad de Oviedo, E-33007 Oviedo, Spain.

[x]Visitor from Texas Tech University, Lubbock, TX 79609, USA.
[y]Visitor from IFIC (CSIC Universitat de Valencia), 56071 Valencia, Spain.
[z]Visitor from Universidad Tecnica Federico Santa Maria, 110v Valparaiso, Chile.
[aa]Visitor from University of Virginia, Charlottesville, VA 22906, USA.
[bb]Yarmouk University, Irbid 211-63, Jordan.
[cc]On leave from J. Stefan Institute, Ljubljana, Slovenia.

[1] $K^{(*)}$ denotes $K^{\pm}$, $K^*(892)^0$, or $K^*(892)^{\pm}$. Charge-conjugate modes are implied throughout this Letter.
[2] T. Hurth and M. Nakao, Annu. Rev. Nucl. Part. Sci. **60**, 645 (2010).
[3] F. Kruger and J. Matias, Phys. Rev. D **71**, 094009 (2005).
[4] U. Egede *et al.*, J. High Energy Phys. 11 (2008) 032.
[5] S. Descotes-Genon *et al.*, J. High Energy Phys. 06 (2011) 099.
[6] C. Bobeth, G. Hiller, and G. Piranishvili, J. High Energy Phys. 07 (2008) 106; W. Altmannshofer *et al.*, J. High Energy Phys. 01 (2009) 019.
[7] B. Aubert *et al.* (*BABAR* Collaboration), Phys. Rev. D **79**, 031102 (2009).
[8] J. T. Wei *et al.* (Belle Collaboration), Phys. Rev. Lett. **103**, 171801 (2009).
[9] T. Aaltonen *et al.* (CDF Collaboration), Phys. Rev. Lett. **106**, 161801 (2011).
[10] T. Aaltonen *et al.* (CDF Collaboration), Phys. Rev. Lett. **107**, 201802 (2011).
[11] K. G. Wilson, Phys. Rev. **179**, 1499 (1969).
[12] C. Bobeth, G. Hiller, and D. van Dyk, J. High Energy Phys. 07 (2010) 098.
[13] A. K. Alok *et al.*, arXiv:1008.2367.
[14] C. Bobeth, G. Hiller, and G. Piranishvili, J. High Energy Phys. 12 (2007) 040.
[15] E. J. Thomson *et al.*, IEEE Trans. Nucl. Sci. **49**, 1063 (2002).
[16] D. Acosta *et al.* (CDF Collaboration), Phys. Rev. D **71**, 032001 (2005).
[17] A. A. Affolder *et al.* (CDF Collaboration), Nucl. Instrum. Methods Phys. Res., Sect. A **526**, 249 (2004).
[18] G. Ascoli *et al.*, Nucl. Instrum. Methods Phys. Res., Sect. A **268**, 33 (1988); T. Dorigo (CDF Collaboration), Nucl. Instrum. Methods Phys. Res., Sect. A **461**, 560 (2001).
[19] We use a cylindrical coordinate system in which θ is the polar angle with respect to the proton beam line and pseudorapidity $\eta \equiv -\ln(\tan\theta/2)$.
[20] T. Aaltonen *et al.* (CDF Collaboration), Phys. Rev. Lett. **102**, 242002 (2009), and references therein.
[21] K. Nakamura *et al.* (Particle Data Group), J. Phys. G **37**, 075021 (2010).
[22] M. Feindt, arXiv:physics/0402093.
[23] See Supplemental Material at http://link.aps.org/supplemental/10.1103/PhysRevLett.108.081807 for angular distributions in each q^2 bin.
[24] We draw theory curves using the EOS code by D. van Dyk *et al.* (http://project.het.physik.tu-dortmund.de/eos/). However, for illustration purposes, we extend these curves into kinematical regions ($q^2 < 1$, $7 < q^2 < 8.68$, $10.09 < q^2 < 12.86$) where their reliability is known to be approximate.